Cell Reports Medicine, Volume *5*

Supplemental information

Alarmin S100A8 imparts chemoresistance of esophageal cancer by reprogramming cancer-associated fibroblasts

Xinjie Chen, Guoyu Cheng, Liang Zhu, Tianyuan Liu, Xinyu Yang, Rucheng Liu, Zhengjie Ou, Shaosen Zhang, Wen Tan, Dongxin Lin, and Chen Wu

Figure S1

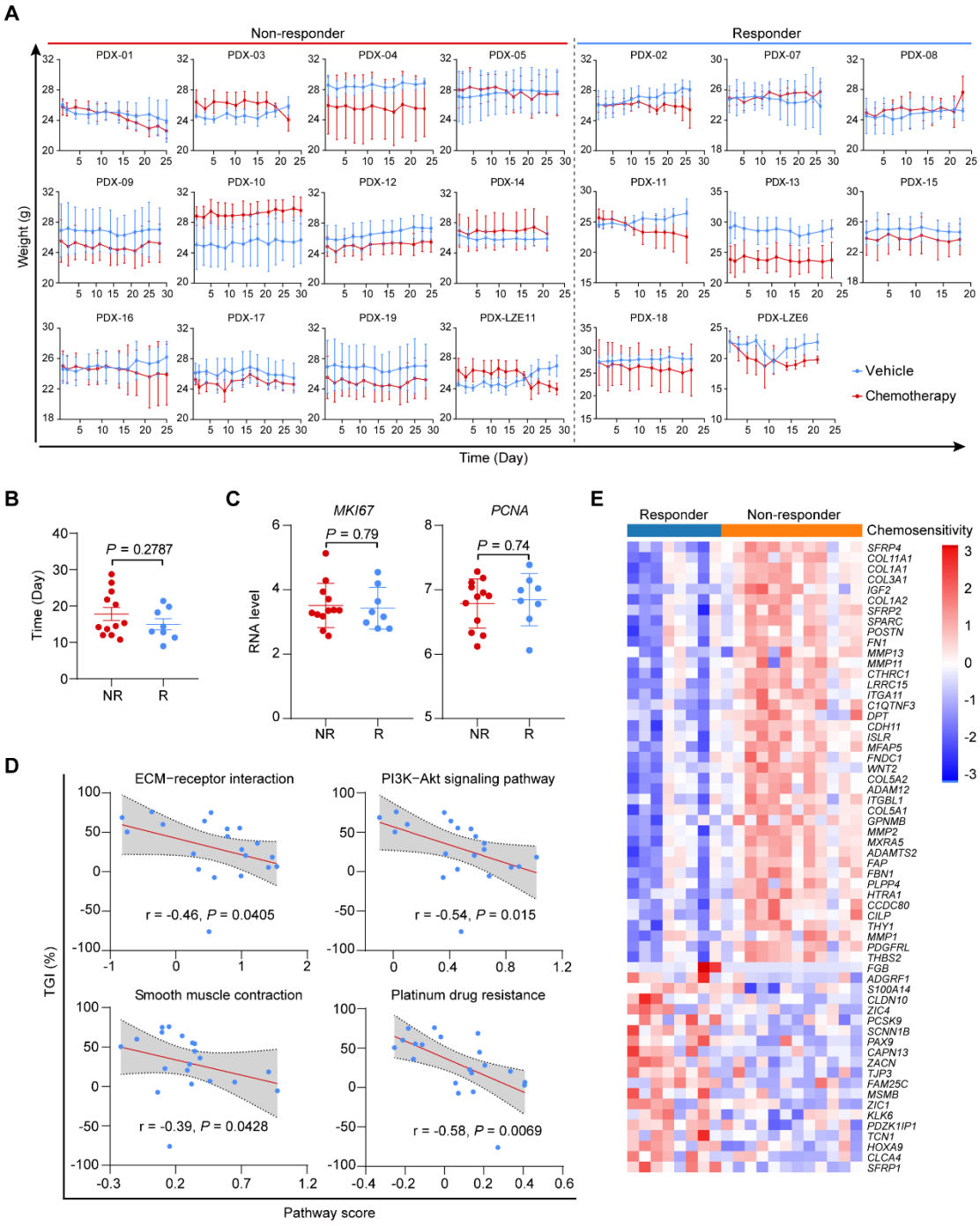

Figure S1. Body weight change, tumor growth rate and additional RNA-seq data analysis in ESCC PDX models. Related to Figure 1.

(A) Body weight curves of PDX mice in chemotherapeutics and vehicle reagents treatment groups (n = 3-5 per group). Data are presented as mean ± SD. (B) Comparison of the number of days that tumor volume in vehicle-treated group grew from 100 to 400 mm^3 between the NR (n = 12) and R (n = 8) groups. Data are presented as mean ± SEM. *P* value is determined by two-tailed Student's t test. (C) Comparison of the RNA level of *MKI67* and *PCNA* between the NR and R groups. Data are presented as mean ± SD. *P* values are determined by two-tailed Student's t test. (D) Spearman correlations between the TGI (%) and the indicated pathway signature scores. The gray areas represent 95%

confidence intervals (n = 20). (E) Heatmap of differentially expressed genes between NR and R groups based on PDX donors' tumor tissues RNA-seq data. Differentially expressed genes between R and NR groups were ordered by fold change.

Figure S2

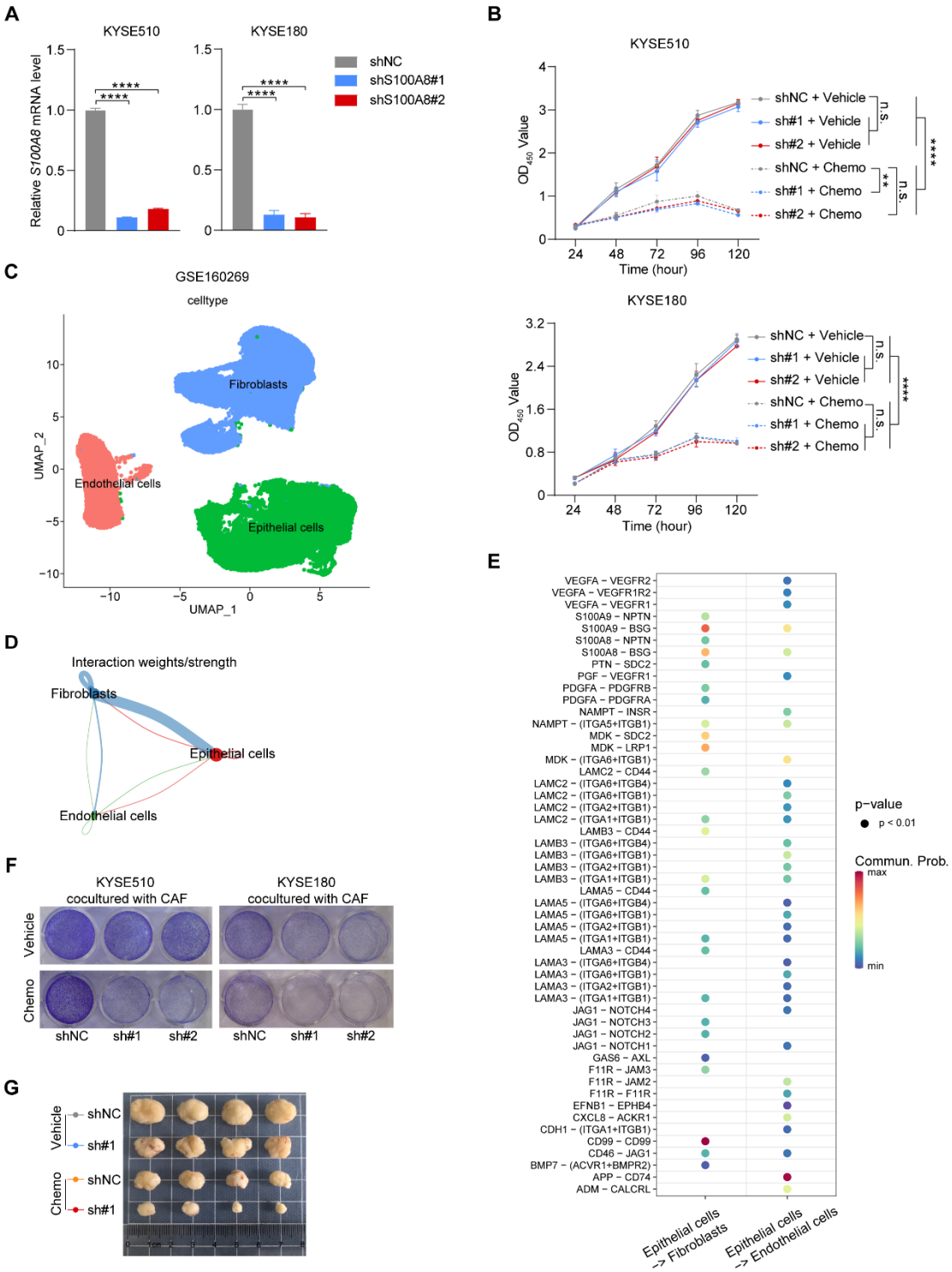

Figure S2. S100A8 confers chemoresistance in a CAF-dependent manner. Related to Figure 2.

(A) Quantitative RT-PCR analysis of *S100A8* in KYSE510 and KYSE180 cells stably transfected with *S100A8* shRNA or control nontargeting shRNA. The expression level was normalized to *GAPDH* (n = 3 biological replicates). (B) Proliferation curves of *S100A8*-knockdown and control cells treated with chemotherapeutics or vehicle (n = 6 biological replicates). (C) Uniform manifold approximation and projection (UMAP) plot of epithelial cells and stromal cells on the basis of their different expression. (D) Ligand-receptor (LR) interactions analysis exhibiting the interaction weights/strength among

epithelial cells, fibroblasts, and endothelial cells. (E) Bubble plot showing interactions of LR gene pairs between epithelial cells and fibroblasts or endothelial cells. (F) Representative images of cell viability of control and *S100A8*- knockdown cells co-cultured with CAFs and treated with chemotherapeutics or vehicle (n = 3 biological replicates). (G) Excised tumor images of control and *S100A8*-knockdown xenografts treated with chemotherapeutics or vehicle reagents (n = 4 per group). For all panels, data are presented as mean ± SD. **$p < 0.01$, ****$p < 0.0001$, and n.s., not significant of two-tailed Student's t test.

Figure S3

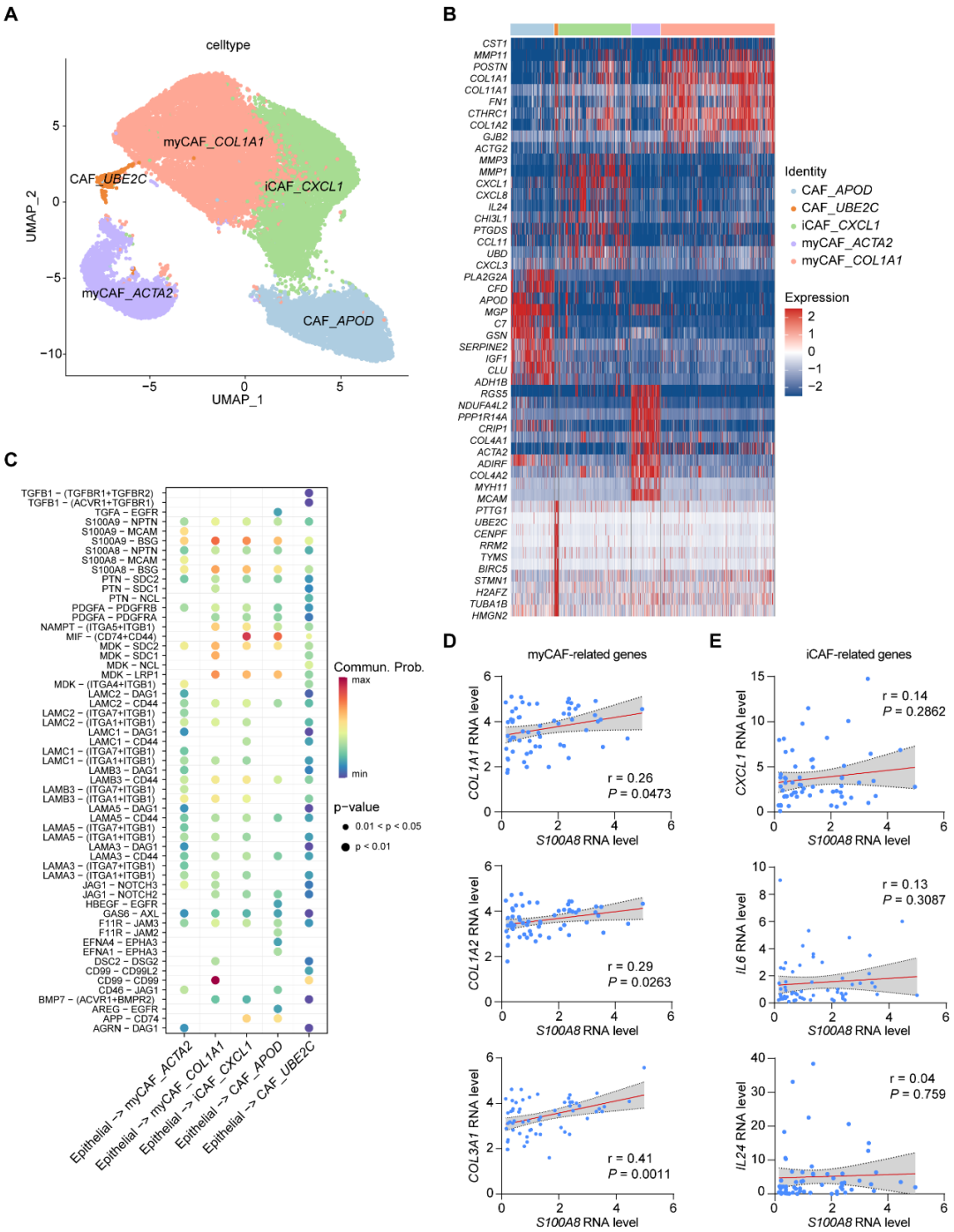

Figure S3. S100A8 expression is associated with myCAFs activation. Related to Figure 3.

(A) UMAP plot of fibroblasts on the basis of their different expression. (B) Heatmap of scaled normalized expression level of the top 10 highly expressed genes for each fibroblast subtype. (C) Bubble plot showing interaction of LR gene pairs between epithelial cells and distinct fibroblast subtypes. (D) Spearman correlations between the *S100A8* RNA level of epithelial cells and the *COL1A1*, *COL1A2*, and *COL3A1* RNA level of fibroblasts. The gray areas represent 95% confidence intervals (n = 60). (E) Spearman correlations between the *S100A8* RNA level of epithelial cells and the *CXCL1*, *IL6*, and *IL24* RNA level of fibroblasts. The gray areas represent 95% confidence intervals (n = 60).

Figure S4

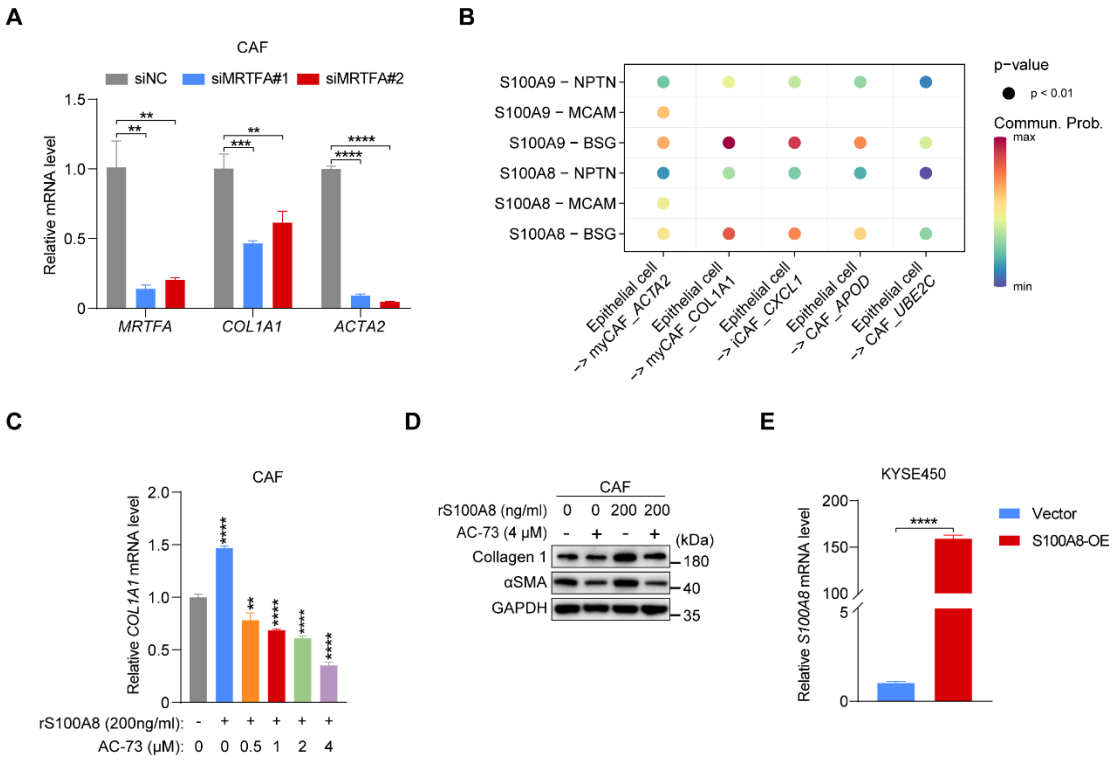

Figure S4. S100A8 activates myCAFs by binding to the CD147 receptor. Related to Figure 4.
(A) Quantitative RT-PCR analysis of *MRTFA*, *COL1A1*, and *ACTA2* in CAFs transfected with *MRTFA* siRNA or control siRNA. The expression level was normalized to GAPDH (n = 3 biological replicates). (B) Bubble plot showing interaction of LR gene pairs between S100A8 in epithelial cells and distinct fibroblast subtypes. (C) Quantitative RT-PCR analysis of *COL1A1* in CAFs treated with or without rS100A8 proteins and treated with indicated concentration of AC-73. The expression level was normalized to GAPDH (n = 3 biological replicates). (D) Western blot analysis of the indicated proteins in CAFs treated with rS100A8 proteins or AC-73. (E) Quantitative RT-PCR analysis of *S100A8* RNA level in control and *S100A8*-overexpression (OE) KYSE450 cells. The expression level was normalized to GAPDH (n = 3 biological replicates). For all panels, data are presented as mean ± SD. **p < 0.01, ***p < 0.001, and ****p < 0.0001 of two-tailed Student's t test.

Figure S5

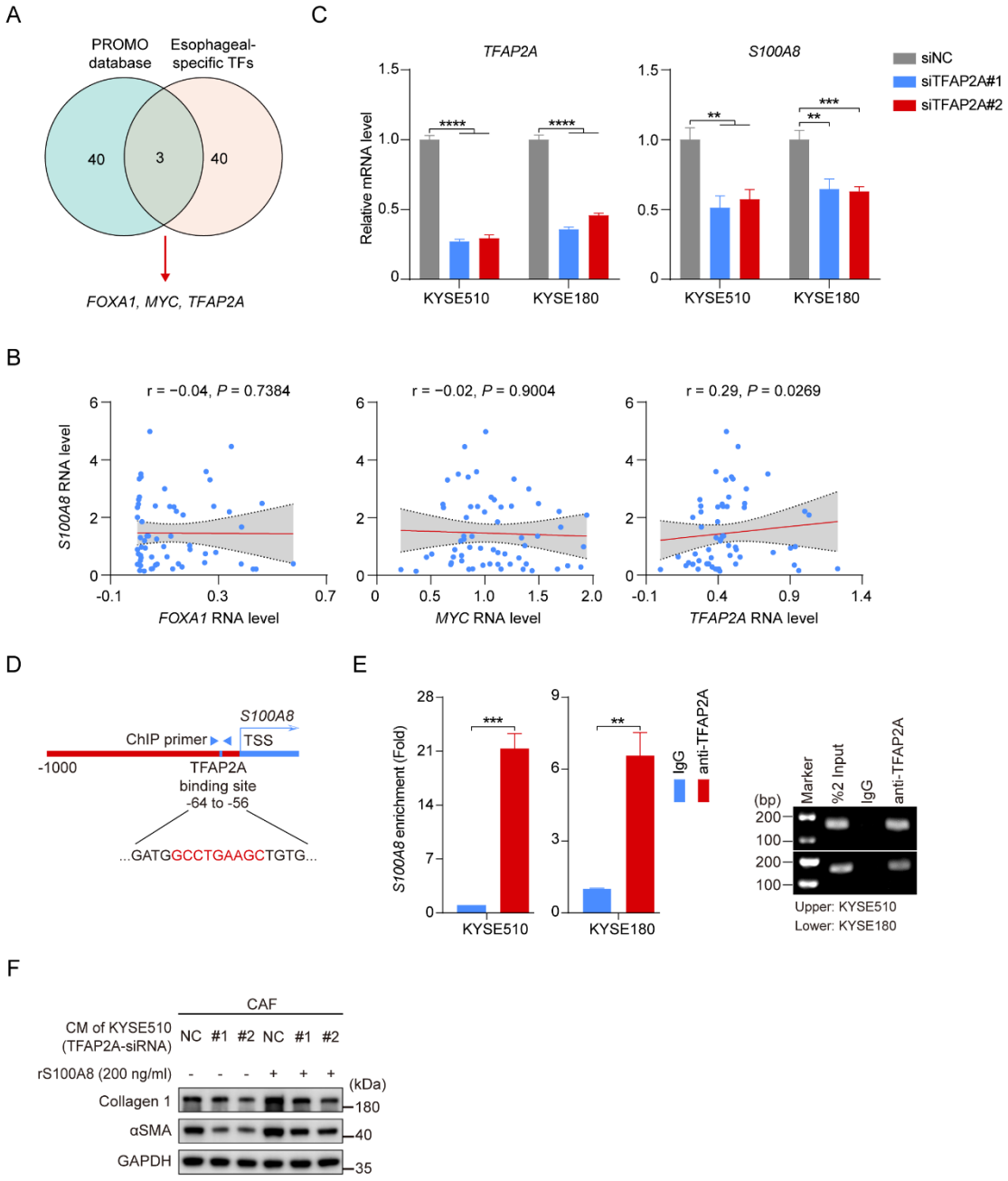

Figure S5. The expression of *S100A8* is regulated by the esophageal-specific transcription factor TFAP2A. Related to Figure 4.

(A) *In silico* analysis of potential transcription factors in *S100A8* promoter region. (B) Spearman correlation between expression levels of candidate transcription factors and *S100A8* RNA level in epithelial cells. The gray areas represent 95% confidence intervals (n = 60). (C) Quantitative RT-PCR analysis of *TFAP2A* and *S100A8* in ESCC cells transfected with *TFAP2A* siRNA or control siRNA. The expression level was normalized to GAPDH (n = 3 biological replicates). (D) Schema of the putative TFAP2A binding site in *S100A8* promoter and the primers used for chromatin immunoprecipitation (ChIP) analysis. Highlighted in red is the predicted motif for TFAP2A binding. (E) ChIP-qPCR analysis of ESCC cells incubated with anti-TFAP2A antibody and IgG control. Left panel showing the qPCR results and the right panel showing the images of agarose gel electrophoresis of the qPCR

products. Data are mean ± SEM. *P* values are determined using two-tailed Student's t test. (F) Western blot analysis of myCAF-related protein markers in CAFs treated with the CM of KYSE510 cells with or without *TFAP2A* knockdown and treated with rS100A8 proteins or PBS. For all panels, **p < 0.01, ***p < 0.001, and ****p < 0.0001 of two-tailed Student's t test.

Figure S6

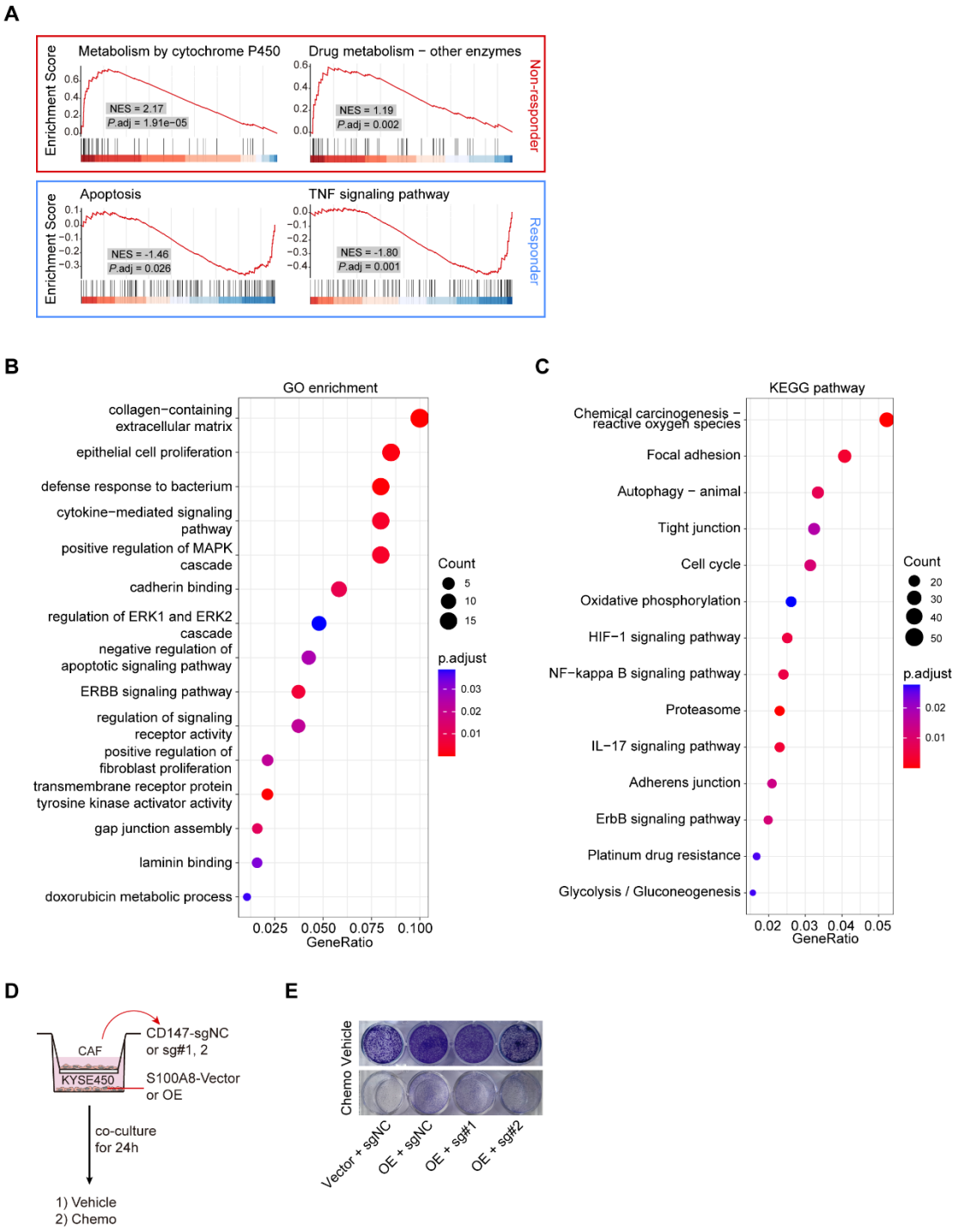

Figure S6. Activated myCAFs endow ESCC cells to acquire chemotherapy resistance by activating anti-apoptotic pathways. Related to Figure 5.

(A) GSEA of pathways enriched in the NR or R group, using RNA-seq data of the PDX mice's tumor tissues. (B and C) Dot plots showing the GO enrichment (B) and KEGG pathway enrichment (C) results of differentially expressed genes in the NR group, using RNA-seq data of the PDX mice's tumor tissues. (D) Schema of co-culture system and cell viability assay. (E) Representative images of cell viability of control and *S100A8*-overexpression KYSE450 cells cocultured with control or CD147-knockout ECAFs and treated with chemotherapeutics or vehicle (n = 3 biological replicates).

Figure S7

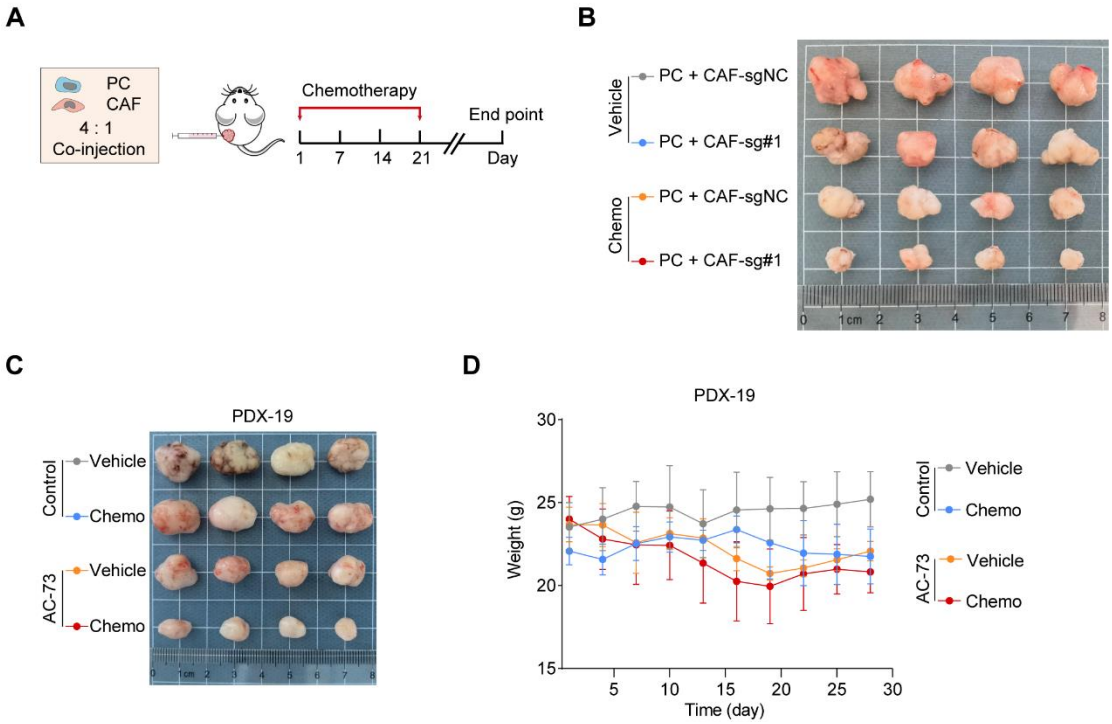

Figure S7. Inhibition of S100A8-CD147 pathway circumvents chemoresistance. Related to Figure 6.

(A) Schema of *in vivo* co-injection and chemosensitivity assays. (B) Excised tumor images of xenografts derived from co-transplantation of control and CD147-knockout CAFs with PCs and treated with chemotherapeutics or vehicle reagents (n = 4 per group). (C) Excised tumor images of xenografts of PDX-19 treated with AC-73 and control solvent and with chemotherapeutics or vehicle reagents (n = 4 per group). (D) Body weight curves of mice treated with AC-73 and control solvent and with chemotherapeutics or vehicle (n = 4 per group). Data are presented as mean ± SD.

Figure S8

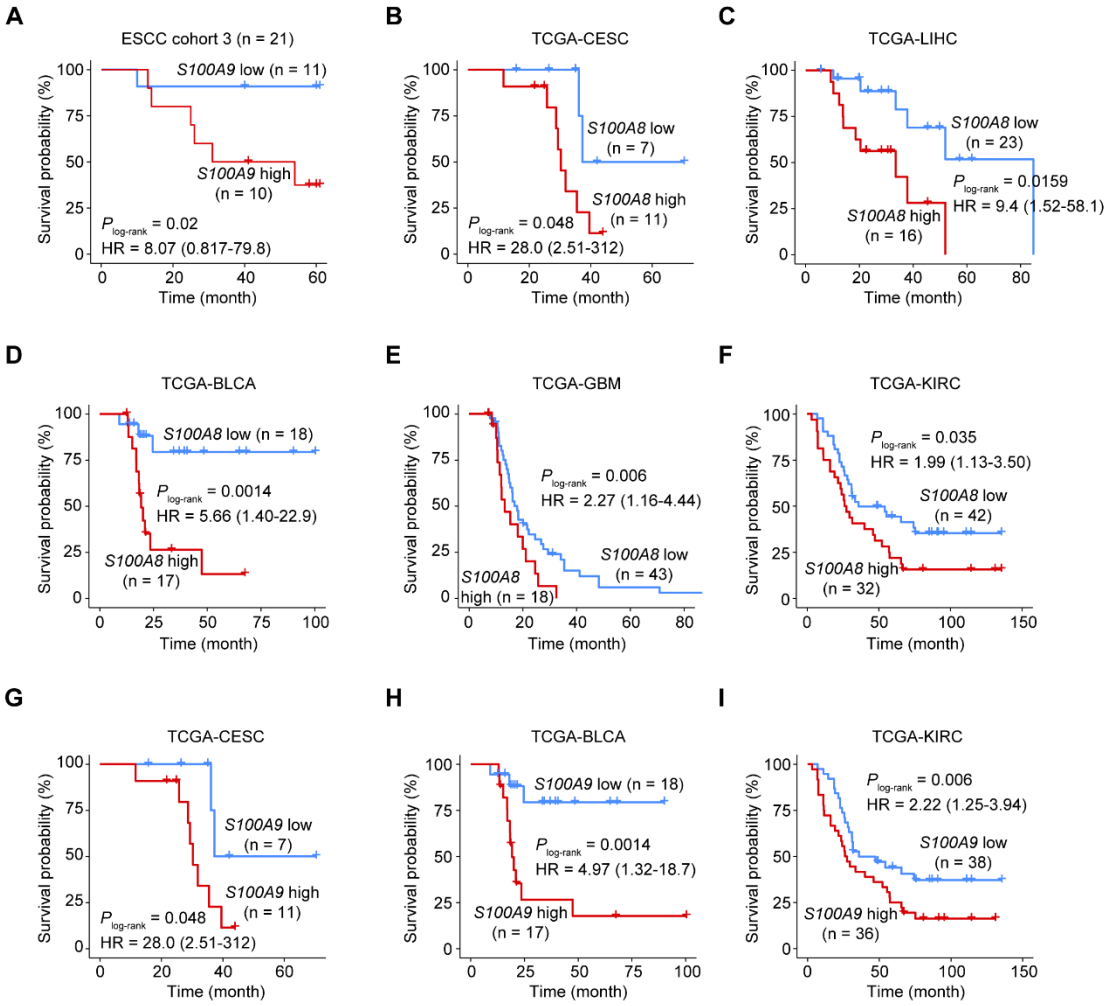

Figure S8. S100A8 serves as a prognostic biomarker for predicting chemotherapy responsiveness. Related to Figure 7.

(A) Kaplan–Meier plot comparing the overall survival (OS) of patients with ESCC treated with chemotherapy with low or high *S100A9* RNA level. Hazard ratio (HR) and 95% confidence interval (CI) are calculated by Cox proportional hazards model with age, gender, and tumor stage as covariates. (B-F) Kaplan–Meier plot comparing the overall survival (OS) of patients with CESC (B), LIHC (C), BLCA (D), GBM (E), and KIRC (F) treated with chemotherapy from TCGA with low or high *S100A8* RNA level. HR and 95% CI are calculated by Cox proportional hazards model with age, gender, and tumor stage as covariates. (G-I) Kaplan–Meier plot comparing the overall survival (OS) of patients with CESC (G), BLCA (H), and KIRC (I) treated with chemotherapy from TCGA with low or high *S100A9* RNA level. HR and 95% CI are calculated by Cox proportional hazards model with age, gender, and tumor stage as covariates.

Table S1. Clinical information of 20 ESCC PDX donors. Related to STAR Methods.

Patient ID	PDX ID	Gender[a]	Age (year)	TNM stage[b]	Location
T633	PDX-01	M	66	III	middle
T638	PDX-02	M	53	II	middle
T623	PDX-03	F	65	III	lower
T649	PDX-04	M	47	II	middle
T616	PDX-05	M	68	III	middle
T622	PDX-07	M	63	III	middle
T611	PDX-08	M	72	III	middle
T814	PDX-09	M	73	II	middle
T643	PDX-10	M	56	II	upper
T629	PDX-11	M	61	II	middle
T621	PDX-12	M	69	II	middle
T634	PDX-13	M	47	III	lower
T620	PDX-14	M	62	III	lower
T642	PDX-15	F	83	I	lower
T648	PDX-16	M	61	III	middle
T650	PDX-17	M	63	II	upper
T646	PDX-18	F	61	II	upper
T618	PDX-19	F	70	III	lower
T624	PDX-20	F	52	II	middle
T645	PDX-21	M	62	III	lower

[a]M, male; F, female.

[b]Tumor TNM staging components including tumor (T), lymph node (N) and metastasis (M) were reviewed by 3 pathologists and defined according to the American Joint Committee on Cancer (AJCC) 7th edition.

Table S3. Clinical information of patients in ESCC cohort 3. Related to Figure 7.

Patient ID	Gender[a]	Age (year)	TNM stage[b]	Survival status[c]	Survival time[d]	Smoking status	Drinking status
P10T	M	62	II	0	61	Smoker	Non-drinker
P126T	M	57	III	1	14	Smoker	Drinker
P127T	M	71	III	0	58	Smoker	Non-drinker
P12T	M	72	II	0	61	Smoker	Non-drinker
P19T	F	40	II	0	41	Non-smoker	Non-drinker
P24T	M	54	III	0	61	Smoker	Drinker
P27T	M	66	II	0	61	Smoker	Drinker
P32T	M	61	II	0	61	Smoker	Drinker
P39T	M	61	III	1	10	Smoker	Non-drinker
P40T	M	61	III	1	31	Smoker	Non-drinker
P42T	M	56	II	0	60	Smoker	Drinker
P47T	M	47	III	1	13	Smoker	Drinker
P57T	M	58	III	0	61	Smoker	Drinker
P74T	M	74	II	1	54	Smoker	Drinker
P76T	M	77	I	0	61	Smoker	Drinker
P80T	F	77	III	1	26	Non-smoker	Non-drinker
P82T	M	72	I	0	40	Smoker	Drinker
P83T	M	59	IV	1	25	Smoker	Drinker
P87T	M	54	III	0	60	Smoker	Drinker
P91T	M	47	II	0	60	Smoker	Drinker
P94T	M	69	III	0	61	Smoker	Non-drinker

[a]M, male; F, female.

[b]Tumor TNM staging components including tumor (T), lymph node (N) and metastasis (M) were defined according to the AJCC 7th edition.

[c]Survival status: 0, alive or lost to follow-up; 1, dead.

[d]The unit of survival time is the month.

Table S4. Sequences of siRNAs, shRNAs, and sgRNAs used in this study. Related to STAR Methods.

Target	Used for	Sequence (5'- 3')
RHOA	siRNA#1	GUACAUGGAGUGUUCAGCAAA
	siRNA#2	UGGAAAGACAUGCUUGCUCAU
ROCK1	siRNA#1	CGGGUUGUUCAGAUUGAGAAA
	siRNA#2	GCACCAGUUGUACCCGAUUUA
MLC2	siRNA#1	CGCCAAGGAUAAAGACGACUA
	siRNA#2	CAUUGAUAAGAAAGGCAACUU
MRTF-A	siRNA#1	GCUGAAGAGAGCCAGACUA
	siRNA#2	CCUGUUUGACAUUCUCAUU
TFAP2A	siRNA#1	CCGCCAUCCCUAUUAACAA
	siRNA#2	CCCAAUGAGCAAGUGACAA
S100A8	shRNA#1	TCAACACTGATGGTGCAGTTA
	shRNA#2	GTGTCCTCAGTATATCAGGAA
CD147	sgRNA#1	GTCGTCAGAACACATCAACG
	sgRNA#2	GGTGGACTCCGACGACCAGT

Table S5. Sequences of primers used in this study. Related to STAR Methods.

Gene	Direction	Sequence
GAPDH	Forward	CGGATTTGGTCGTATTGGGC
	Reverse	TGATTTTGGAGGGATCTCGC
TFAP2A	Forward	AGGTCAATCTCCCTACACGAG
	Reverse	GGAGTAAGGATCTTGCGACTGG
S100A8 (RT-qPCR)	Forward	ATGCCGTCTACAGGGATGAC
	Reverse	CCACGCCCATCTTTATCACC
S100A8 promoter (ChIP-qPCR)	Forward	TTCATTCTGCACAGTGATTGCCA
	Reverse	GAGGCAGCTCCTTTTTATAGCG
COL1A1	Forward	GAGGGCCAAGACGAAGACATC
	Reverse	CAGATCACGTCATCGCACAAC
ACTA2	Forward	CTATGAGGGCTATGCCTTGCC
	Reverse	GCTCAGCAGTAGTAACGAAGGA